The Journal of Chemical Physics

Elastic properties of self-assembled bilayer membranes: Analytic expressions via asymptotic expansion

Cite as: J. Chem. Phys. **152**, 244121 (2020); https://doi.org/10.1063/5.0009734
Submitted: 02 April 2020 . Accepted: 09 June 2020 . Published Online: 26 June 2020

Yongqiang Cai, Sirui Li, and An-Chang Shi

The Journal of Chemical Physics ARTICLE scitation.org/journal/jcp

Elastic properties of self-assembled bilayer membranes: Analytic expressions via asymptotic expansion

Cite as: J. Chem. Phys. 152, 244121 (2020); doi: 10.1063/5.0009734
Submitted: 2 April 2020 • Accepted: 9 June 2020 •
Published Online: 26 June 2020

Yongqiang Cai,[1,a)] Sirui Li,[2,3] and An-Chang Shi[4]

AFFILIATIONS

[1]Department of Mathematics, National University of Singapore, 21 Lower Kent Ridge Road, Singapore 119077, Singapore
[2]School of Mathematics and Statistics, Guizhou University, Huaxi District, Guiyang 550025, People's Republic of China
[3]School of Mathematical Sciences, Zhejiang University, 886 Yuhang Road Xihu District, Hangzhou 310027, People's Republic of China
[4]Department of Physics and Astronomy, McMaster University, 1280 Main Street West, Hamilton, Ontario L8S 4M1, Canada

[a)]**Author to whom correspondence should be addressed:** caiyq.math@foxmail.com

ABSTRACT

Bilayer membranes self-assembled from amphiphilic molecules are ubiquitous in biological and soft matter systems. The elastic properties of bilayer membranes are essential in determining the shape and structure of bilayers. A novel method to calculate the elastic moduli of the self-assembled bilayers within the framework of the self-consistent field theory is developed based on an asymptotic expansion of the order parameters in terms of the bilayer curvature. In particular, the asymptotic expansion method is used to derive analytic expressions of the elastic moduli, which allows us to design more efficient numerical schemes. The efficiency of the proposed method is illustrated by a model system composed of flexible amphiphilic chains dissolved in hydrophilic polymeric solvents.

I. INTRODUCTION

The self-assembly of amphiphilic molecules to form cellular membranes is a fundamental process in biological systems. At the same time, self-assembled bilayer membranes and polymersomes[1,2] from amphiphilic macromolecules are abundant in soft matter systems. In particular, the self-assembled bilayers from amphiphilic polymers such as block copolymers could act as mimetics to biological membranes. Because there are virtually no limits to the combinations of monomers, polymeric hybrid materials show great promise for applications in biomedicine and biotechnology.[3] Phenomenologically, a membrane could be modeled as a two-dimensional surface S, whose mechanical properties could be used to understand the formation and stability of membrane morphologies. When the curvature of the membrane is small, its deformation energy could be described by Helfrich's linear elasticity theory.[4,5] However, when the curvature is large, higher-order contributions to the membrane's free energy become significant. Specifically, the elastic energy includes fourth-order contributions of a closed membrane and is given by

$$F = \int_S \left[\gamma + 2\kappa_M (M - c_0)^2 + \kappa_G G + \kappa_1 M^4 + \kappa_2 M^2 G + \kappa_3 G^2\right] dA, \quad (1)$$

where $M = (c + c')/2$ and $G = cc'$ are the local mean and Gaussian curvatures of a deformed bilayer, respectively (c and c' are the two principal curvatures). The linear elastic energy of a bilayer is specified by the elastic constants, γ, c_0, κ_M, and κ_G, corresponding to the surface tension, spontaneous curvature, bending modulus, and Gaussian modulus, respectively. In addition, κ_1, κ_2, and κ_3 are the fourth-order curvature moduli. It should be noted that the spontaneous curvature c_0 is zero and the third-order terms are not included in Eq. (1) due to the symmetry of the bilayers. Usually, the expansion of free energy is truncated to second-order in curvatures, which is the so-called Helfrich model.[4,5] In contrast, the fourth-order terms are less considered since they are relevant to each other, and in turn, it is more difficult to determine their coefficients, κ_1, κ_2,and κ_3.

In the last few decades, a number of experimental techniques,[6,7] simulation methods,[8–11] and theoretical methods[12–14] have been developed to obtain the elastic constants of bilayer membranes. Theoretically, the elastic constants can be obtained by studying bilayers in different geometries (e.g., planes, cylinders, and spheres) and then comparing the free energy of membranes with the corresponding expressions derived from elasticity theories.[13] The elastic constants could then be extracted by fitting the theoretical expressions to the computed free energy curves. This approach can be implemented quite naturally in theoretical studies. However, this numerical approach requires an accurate computation of the free energy of curved membranes.

Among the different theoretical frameworks developed for amphiphilic molecules, the self-consistent field theory (SCFT) provides a versatile platform for the study of the self-assembled bilayer membranes. Several studies using the SCFT have been carried out to study the elastic properties of bilayers,[13,15–17] where the polymers are assumed to be flexible, and the Gaussian polymer model is used to describe the blocks. Using similar theoretical approaches, Ref. 18 compared the elastic properties between the triblock membranes and the diblock membranes, and Ref. 19 extended this approach to the semiflexible chain model described by the wormlike-chain to study the elastic properties of semiflexible bilayers. These previous studies firmly established that the SCFT provides a flexible and accurate framework for the study of inhomogeneous polymeric systems, including different micelle structures[20,21] and bilayer membranes.[17–19]

In previous studies,[17–19] the excess free energy of the bilayer membrane in different geometries, such as infinite planar, cylindrical and spherical bilayers with different curvatures, was computed. The excess free energy of the three geometries, which is denoted by F^0, F^C, and F^S for the planar, cylindrical, and spherical bilayers, respectively, was then used to extract the elastic constants of the membranes. Specifically, the expressions of the free energy of the membranes with different shapes are obtained from the Helfrich model [Eq. (1)]. In particular, the free energies, F^C and F^S, are polynomials with respect to the principal curvature c, where the coefficients are combinations of the elastic constants. As a result, the elastic moduli, such as κ_M and κ_G, could be obtained by quadratic polynomial fitting F^C and F^S as functions of c. However, there are two drawbacks of this strategy: (i) the fitting range of $c \in (0, c_{max})$ should be carefully chosen since higher-order energies are not negligible when c is large and (ii) accurate fitting requires the computation of the bilayer energy as a function of curvature, which, in turn, requires solving the self-consistent field (SCF) equations many times. In order to overcome these drawbacks, new methods to obtain elastic moduli are desirable.

In this paper, we propose an asymptotic expansion method within the SCFT framework to calculate the elastic moduli of the self-assembled bilayer membranes. It should be noted that generalization of the expansion method to other free energy functionals is straightforward. Similar expansions had been derived for free energy functionals based on the packing constraints,[22] Ginzburg–Landau model,[23] and van der Waals theory.[24] Specifically, we treat the curvature of cylindrical and spherical bilayers as a small parameter and carry out an asymptotic expansion of the free energy in terms of the curvature. Analytical expressions of the free energy at each order are obtained, so they could be computed separately. In particular, computation of the elastic moduli only requires the solution of a few SCF equations. Besides, more accurate numerical schemes could be developed to solve the SCF equations. Numerically, the elastic moduli obtained by using the asymptotic expansion method are consistent with those obtained by the fitting method. From the theoretical viewpoint, the asymptotic expansion results directly relate the elastic moduli to the equilibrium distribution of the amphiphilic molecules, thus providing an understanding of the dependence of elastic properties on molecular details.

The remainder of this paper is organized as follows: Section II describes the SCFT model of bilayer membranes and the geometric constraints used in this study. Section III gives the asymptotic expansion method where the corresponding modified diffusion equations (MDEs) and SCF equations are given. Section IV gives the numerical method for solving the whole SCFT model. Our results on the elastic properties of the membranes are presented in Sec. V, including the influence of microscopic parameters of the flexible–flexible system on the elastic properties. Finally, Sec. VI concludes with a brief summary.

II. THEORETICAL MODEL AND GEOMETRY CONSTRAINTS

A. Molecular model

The molecular model used in this study is a binary mixture of AB-diblock copolymers and A-homopolymers. This is a generic model in which the amphiphilic molecules are modeled by the AB-diblock copolymers, whereas the amphiphilic solvent molecules are modeled by the A-homopolymers. Furthermore, the polymeric species are modeled as flexible Gaussian chains. We assume that the A/AB blend is incompressible, and both monomers (A and B) have the same monomeric density ρ_0 (or the hardcore volume per monomer is ρ_0^{-1}). The diblock copolymers and homopolymers are characterized by their degrees of polymerization, N and $N_h \equiv f_h N$, respectively. The volume fraction of the A- and B-blocks in the copolymers is denoted by f_A and $f_B = 1 - f_A$, respectively. The radius of gyration of A and B blocks is denoted by $R_g^A = \sqrt{f_A N l_a^2/6}$ and $R_g^B = \sqrt{f_B N l_b^2/6}$, where l_a and l_b are the statistical segment length of A and B monomers, respectively. We set $R_g := \sqrt{N l_a^2/6}$ as the unit spatial length in nondimensionalization and define $a = l_a/l_a = 1$ as a constant and $b = l_b/l_a$ as the geometrical parameter describing the conformational asymmetry of the A and B blocks. The interaction between the A and B monomers is described by a Flory–Huggins parameter[25] χ. Finally, the chemical potential of the copolymers μ_c, or the corresponding activity $z_c = \exp(\mu_c)$, is used to control the average concentration of the diblock copolymers in the blends.

Within the SCFT framework formulated in the grand canonical ensemble,[17,20,26] the free energy of the binary mixture is given by

$$\frac{N\mathscr{F}}{k_B T \rho_0} = \int d\mathbf{r}[\chi N \phi_A(\mathbf{r})\phi_B(\mathbf{r}) - \omega_A(\mathbf{r})\phi_A(\mathbf{r}) - \omega_B(\mathbf{r})\phi_B(\mathbf{r}) - \xi(\mathbf{r})(\phi_A(\mathbf{r}) + \phi_B(\mathbf{r}) - 1) + \psi G_\varepsilon(\mathbf{r} - \mathbf{r}_1)(\phi_A(\mathbf{r}) - \phi_B(\mathbf{r}))] - z_c Q_c - Q_h, \quad (2)$$

where $\phi_\alpha(\mathbf{r})$ and $\omega_\alpha(\mathbf{r})$ are the local concentration and the mean field of the α-type monomers (α = A, B), respectively. The local pressure $\xi(\mathbf{r})$ is a Lagrange multiplier introduced to enforce incompressibility of the system. A second Lagrange multiplier, ψ, is used to ensure the constraints for stabilizing the bilayer in different geometries, where a sharp Gaussian function, $G_\varepsilon(\mathbf{r}-\mathbf{r}_1)$, is used to ensure that the ψ field only operates near the interface at a prescribed position $\mathbf{r}_1$. The last two terms in Eq. (2) are the contributions from the single-chain partition functions of the two polymers, Q_c and Q_h. Note that, in previous studies,[17,27] a constraint term, $\delta(\mathbf{r}-\mathbf{r}_1)(\phi_A(\mathbf{r})-\phi_B(\mathbf{r}))$, has been included in the free energy functional to stabilize a bilayer in different geometries. In this study, we replace the delta function $\delta(\mathbf{r})$ by the Gaussian function, resulting in the constraint term, $G_\varepsilon(\mathbf{r}-\mathbf{r}_1)(\phi_A(\mathbf{r})-\phi_B(\mathbf{r}))$, in Eq. (2). This modification could make numerical schedules more robust and have negligible effects on the numerical results.

The fundamental quantities to be calculated in the SCFT are the probability distribution functions (or the propagators) of the polymers, i.e.,$q_A^h(\mathbf{r},s)$ for the A-homopolymers and $q_A^\pm(\mathbf{r},s), q_B^\pm(\mathbf{r},s)$ for the AB-diblock copolymers. These propagators are obtained as solutions of the modified diffusion equations (MDEs)[20] in the presence of the mean fields (ω_A and ω_B),

$$\frac{\partial}{\partial s}q_A^h(\mathbf{r},s) = \left(a^2\nabla_{\mathbf{r}}^2 - \omega_A(\mathbf{r})\right)q_A^h(\mathbf{r},s), \quad s\in(0,f_h), \tag{3}$$

$$\frac{\partial}{\partial s}q_A^\pm(\mathbf{r},s) = \left(a^2\nabla_{\mathbf{r}}^2 - \omega_A(\mathbf{r})\right)q_A^\pm(\mathbf{r},s), \quad s\in(0,f_A), \tag{4}$$

$$\frac{\partial}{\partial s}q_B^\pm(\mathbf{r},s) = \left(b^2\nabla_{\mathbf{r}}^2 - \omega_B(\mathbf{r})\right)q_B^\pm(\mathbf{r},s), \quad s\in(0,f_B) \tag{5}$$

with the initial value conditions,

$$q_A^h(\mathbf{r},0) = q_A^-(\mathbf{r},0) = q_B^-(\mathbf{r},0) = 1,$$

$$q_A^+(\mathbf{r},0) = q_B^-(\mathbf{r},f_B),$$

$$q_B^+(\mathbf{r},0) = q_A^-(\mathbf{r},f_A).$$

In terms of the chain propagators, the single-chain partition functions are given by

$$Q_c = \int d\mathbf{r}q_A^+(\mathbf{r},f_A), \tag{6}$$

$$Q_h = \int d\mathbf{r}q_A^h(\mathbf{r},f_h). \tag{7}$$

Furthermore, the local concentrations of the A and B monomers are obtained from the propagators as

$$\phi_A(\mathbf{r}) = \phi_A^h + \phi_A^c = \int_0^{f_h} ds q_A^h(\mathbf{r},s)q_A^h(\mathbf{r},f_h-s) + z_c\int_0^{f_A} ds q_A^-(\mathbf{r},s)q_A^+(\mathbf{r},f_A-s), \tag{8}$$

$$\phi_B(\mathbf{r}) = z_c\int_0^{f_B} ds q_B^-(\mathbf{r},s)q_B^+(\mathbf{r},f_B-s). \tag{9}$$

The rest of the SCF equations concerning the mean fields to the local concentrations are

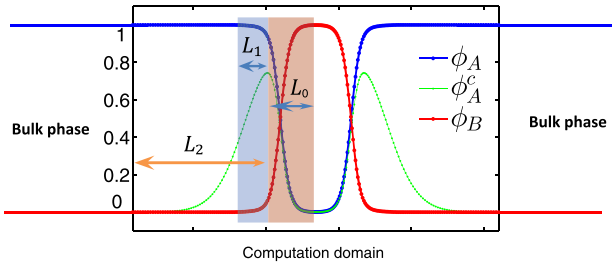

FIG. 1. Profile of the bilayer structure. The computation domain is truncated to make sure that the order near the boundary is close to the bulk phase.

$$\omega_A(\mathbf{r}) = \chi N\phi_B(\mathbf{r}) - \xi(\mathbf{r}) + \psi G_\varepsilon(\mathbf{r}-\mathbf{r}_1), \tag{10}$$

$$\omega_B(\mathbf{r}) = \chi N\phi_A(\mathbf{r}) - \xi(\mathbf{r}) - \psi G_\varepsilon(\mathbf{r}-\mathbf{r}_1), \tag{11}$$

$$\phi_A(\mathbf{r}) + \phi_B(\mathbf{r}) = 1, \tag{12}$$

$$\int d\mathbf{r}G_\varepsilon(\mathbf{r}-\mathbf{r}_1)(\phi_A(\mathbf{r})-\phi_B(\mathbf{r})) = 0. \tag{13}$$

The set of Eqs. (2)–(13) form the self-consistent theory of the model. It should be noted that the SCF equations are highly nonlinear and nonlocal; thus, they could have many solutions. In this study, we will focus on the solutions corresponding to a bilayer whose profile is shown in Fig. 1. Furthermore, we are interested in the free energy of a system containing a bilayer membrane compared to that of the homogeneous bulk phase $\mathscr{F}_{bulk}$, which can be computed analytically using the constant solution of the SCF equations.[17,26] The free energy difference $(\mathscr{F}-\mathscr{F}_{bulk})$ is proportional to the area of the membrane A; therefore, we can define an excess free energy density by

$$F_{ex} = \frac{N(\mathscr{F}-\mathscr{F}_{bulk})}{k_BT\rho_0 A}. \tag{14}$$

The corresponding free energy density for the bulk phase is given by

$$f_{bulk} := \frac{N\mathscr{F}_{bulk}}{k_BT\rho_0 V} = \frac{1}{f_h}\left(\ln\left(\frac{1-\phi_{bulk}}{f_h}\right)+\phi_{bulk}-1\right)+\chi N f_B^2\phi_{bulk}^2-\phi_{bulk}, \tag{15}$$

where the bulk copolymer concentration ϕ_{bulk} is determined by the following equation:

$$\mu_c = \ln\phi_{bulk} - \frac{1}{f_h}\ln\left(\frac{1-\phi_{bulk}}{f_h}\right)+\chi N f_B(1-2f_B\phi_{bulk}). \tag{16}$$

Equation (16) for ϕ_{bulk} has at least one solution. In cases where it has more than one solution, the one with the lowest free energy density is chosen as the bulk phase.

B. Geometric constraints and the polynomial fitting method

In order to extract the elastic constants, such as the bending modulus and Gaussian modulus, of the self-assembled bilayers, one

could calculate the excess free energy of a bilayer membrane in three geometries:[13,17] an infinite planar bilayer, a cylindrical bilayer with a radius r (or a mean curvature $M = c/2 = 1/2r$), which is extended to infinity in the cylindrical direction, and a spherical bilayer with a radius r (or a mean curvature $M = c = 1/r$). In the cylindrical and spherical geometries, the constraint $\psi G_\varepsilon(\mathbf{r} - \mathbf{r}_1)$ in Eq. (2) is applied to the outer monolayer where $\mathbf{r}_1$ is set to control the curvature of the self-assembled bilayer. One advantage of those geometries is that the simulation of bilayers with these geometries can be reduced to one-dimensional problems in their corresponding coordinate systems. Specifically, the MDEs (3)–(5) in one-dimensional planar, cylindrical, and spherical coordinate systems could be written in a unified form,

$$\frac{\partial}{\partial s}q(r,s) = a^2\left(\frac{\partial^2}{\partial r^2} + \frac{n}{r}\frac{\partial}{\partial r}\right)q(r,s) - \omega(r)q(r,s), \tag{17}$$

where $n = 0$, 1, and 2 for planar, cylindrical, and spherical coordinate systems, respectively.

The next step of the calculation is to compare the excess free energies, F^0, $F^C(c)$, and $F^S(c)$, of the bilayers with the expressions of the Helfrich model in the corresponding geometries,

$$F^0 = \gamma + 2\kappa_M c_0^2,$$

$$F^C(c) = F^0 - 2\kappa_M c_0 c + \frac{\kappa_M}{2}c^2 + B_C c^4,$$

$$F^S(c) = F^0 - 4\kappa_M c_0 c + (2\kappa_M + \kappa_G)c^2 + B_S c^4,$$

where the parameters $B_C := \kappa_1/16$ and $B_S := \kappa_1 + \kappa_2 + \kappa_3$ are combinations of the fourth-order moduli. In previous studies,[17–19] the bending modulus κ_M, Gaussian modulus κ_G, and higher order moduli B_C and B_S are obtained by a polynomial fitting method. In detail, a series of curvatures $\{c_i\}$ are chosen and then the SCF equations are solved for each curvature c_i to get the energies $\{F^C(c_i)\}$ and $\{F^S(c_i)\}$. After that, the polynomial fitting method is used to obtain the polynomial coefficients, which, in turn, gives the elastic moduli.

While the polynomial fitting method is fine for determining the second-order moduli, it becomes inaccurate when trying to extract higher-order moduli. Specifically, during the polynomial fitting process, two factors will affect the results. The first factor is the size of the set $\{c_i\}$. Since the energies, $F^C(c_i)$ and $F^S(c_i)$, are numerically calculated, which must contain inaccuracies, one needs to choose a large number of c_i (for example, 50 different c_i) to make sure that the fitted higher-order moduli are accurate. This, in turn, requires that one must solve the SCF equations many times (for example, 2 × 50 times). The second factor is in the range of $\{c_i\} \subset (0, c_{max})$. The numerical errors prevent one from choosing small c_{max} since that is where the energies are very close. However, if c_{max} is large, the higher-order terms are not negligible. Therefore, it is not straightforward to choose c_{max} and the number of c_i to make the fitting results reasonable. Those drawbacks of the polynomial fitting method motivated us to develop new schemes to obtain the elastic moduli, especially the higher-order moduli. In Sec. III, we propose a new scheme, based on the asymptotic expansion theory, which not only overcomes the drawbacks of the fitting method but also gives the polynomial coefficients directly and efficiently.

III. ASYMPTOTIC EXPANSION METHOD

Since the curvature of cylindrical and spherical bilayers is assumed to be small, we can regard it as a small parameter for the application of the asymptotic expansion theory.[28,29] In this section, we show that analytic expressions of the MDE, SCF equations, and free energy at each order could be obtained separately.

A. MDE at each order

When the curvature c is small, i.e., r is large, we can perform asymptotic expansions of the MDE with respect to the bilayer curvature. The expansion starts from the coordinate transformation, $r = x - \frac{1}{c}$. With this transformation, we can formally write down the functions $\omega(r)$, $q(r, s)$, and $\frac{1}{r}$ as expansions in terms of the curvature c,

$$\omega(r) = \omega_0(x) + c\omega_1(x) + c^2\omega_2(x) + \cdots, v$$

$$q(r,s) = q_0(x,s) + cq_1(x,s) + c^2q_2(x,s) + \cdots,$$

$$\frac{1}{r} = \frac{1}{x + 1/c} = \frac{c}{1 + cx} = c - xc^2 + x^2c^3 + \cdots.$$

Substitute these expressions in the MDE [Eq. (17)], we obtain

$$\begin{aligned}
&(a^2\nabla^2 - \omega(r))q(r,s)\\
&= \left(a^2\partial_{rr} + \frac{na^2}{r}\partial_r - \omega_0(x) - c\omega_1(x) - c^2\omega_2(x) + \cdots\right)\\
&\quad\times\left(q_0(x,s) + cq_1(x,s) + c^2q_2(x,s) + \cdots\right)\\
&= (a^2\partial_{xx}^2 - \omega_0)q_0 + \left[(a^2\partial_{xx}^2 - \omega_0)q_1 + (na^2\partial_x - \omega_1)q_0\right]c\\
&\quad + \left[(a^2\partial_{xx}^2 - \omega_0)q_2 + (na^2\partial_x - \omega_1)q_1\right.\\
&\quad \left. + (-na^2x\partial_x - \omega_2)q_0\right]c^2 + \cdots.
\end{aligned}$$

Comparing the terms with different order of c, we can write down the MDE at each order as

$$\partial_s q_i(x,s) = \sum_{j=0}^{i} L_j q_{i-j}(x,s), \quad i = 0, 1, 2, \ldots, \tag{18}$$

where L_j are derivative operators defined by

$$L_0 = a^2\partial_{xx}^2 - \omega_0, \quad L_j = na^2(-x)^{j-1}\partial_x - \omega_j, \quad j \geq 1. \tag{19}$$

In particular, the MDEs up to the second-order in c are given by

$$\partial_s q_0 = (a^2\partial_{xx}^2 - \omega_0)q_0,$$

$$\partial_s q_1 = (a^2\partial_{xx}^2 - \omega_0)q_1 + (na^2\partial_x - \omega_1)q_0,$$

$$\partial_s q_2 = (a^2\partial_{xx}^2 - \omega_0)q_2 + (na^2\partial_x - \omega_1)q_1 + (-na^2x\partial_x - \omega_2)q_0.$$

B. SCF equations at each order

Operating the MDE on the propagators and employing the following initial conditions:

$$q^h_{Ai}(x,0) = q^-_{Ai}(x,0) = q^-_{Bi}(x,0) = \delta_{0i},$$

$$q^+_{Ai}(x,0) = q^-_{Bi}(x,f_B),$$

$$q^+_{Bi}(x,0) = q^-_{Ai}(x,f_A), \quad i = 0,1,2,\ldots,$$

we can get the expansion for the propagators $q^h_A, q^\pm_A$, and $q^\pm_B$,

$$q^h_A(x,s) = \sum_{i\geq 0} c^i q^h_{Ai}(x,s),$$

$$q^\pm_A(x,s) = \sum_{i\geq 0} c^i q^\pm_{Ai}(x,s),$$

$$q^\pm_B(x,s) = \sum_{i\geq 0} c^i q^\pm_{Bi}(x,s).$$

Here, δ_{ij} is the Kronecker delta function, i.e., $\delta_{0i} = 1$ for $i = 0$ and $\delta_{0i} = 0$ for $i \geq 1$. These expressions can then be used to calculate the order parameters expansion at each order,

$$\phi^h_A(x) = \sum_{i\geq 0} c^i \phi^h_{Ai}(x) = \sum_{i\geq 0} c^i \int_0^{f_h} ds \sum_{j=0}^{i} q^h_{Aj}(x,s) q^h_{A,i-j}(x,f_h - s), \tag{20}$$

$$\phi^c_A(x) = \sum_{i\geq 0} c^i \phi^c_{Ai}(x) = \sum_{i\geq 0} c^i z_c \int_0^{f_A} ds \sum_{j=0}^{i} q^-_{Aj}(x,s) q^+_{A,i-j}(x,f_A - s), \tag{21}$$

$$\phi_B(x) = \sum_{i\geq 0} c^i \phi_{Bi}(x) = \sum_{i\geq 0} c^i z_c \int_0^{f_B} ds \sum_{j=0}^{i} q^-_{Bj}(x,s) q^+_{B,i-j}(x,f_B - s). \tag{22}$$

In addition, $\phi_{Ai}(x) = \phi^h_{Ai}(x) + \phi^c_{Ai}(x)$.

The expansion of the SCF equations can be carried out similarly. In the cylindrical and spherical geometries, the constraint $\psi G_\varepsilon(\mathbf{r} - \mathbf{r}_1)$ is applied to the outer monolayer only. It allows the bilayer to optimize its thickness or position h and indirectly set the curvature radius of the membrane. The constraint position r_1 can be characterized by two quantities: one is the curvature radius $\frac{1}{c}$ and another is the relative constraint position $h := r_1 - \frac{1}{c}$, which is a function of c. Let $h = \sum_{i\geq 0} c^i h_i$, then using the Taylor expansion, we have

$$G_\varepsilon(\mathbf{r} - \mathbf{r}_1) = G_\varepsilon(x - h) = \sum_{k\geq 0} \frac{(h_0 - h)^k}{k!} G^{(k)}_\varepsilon(x - h_0) = \sum_{k\geq 0} \frac{(-\sum_{i\geq 1} c^i h_i)^k}{k!} G^{(k)}_\varepsilon(x - h_0) =: \sum_{i\geq 0} c^i G_{\varepsilon,i}(x - h_0),$$

where the leading terms are

$$G_{\varepsilon,0}(x - h_0) = G_\varepsilon(x - h_0),$$

$$G_{\varepsilon,1}(x - h_0) = -h_1 G^{(1)}_\varepsilon(x - h_0),$$

$$G_{\varepsilon,2}(x - h_0) = -h_2 G^{(1)}_\varepsilon(x - h_0) + \frac{h_1^2}{2} G^{(2)}_\varepsilon(x - h_0),$$

$$G_{\varepsilon,3}(x - h_0) = -h_3 G^{(1)}_\varepsilon(x - h_0) + h_1 h_2 G^{(2)}_\varepsilon(x - h_0) - \frac{h_1^3}{6} G^{(3)}_\varepsilon(x - h_0),$$

$$G_{\varepsilon,4}(x - h_0) = -h_4 G^{(1)}_\varepsilon(x - h_0) + \frac{2h_1 h_3 + h_2^2}{2} G^{(2)}_\varepsilon(x - h_0) - \frac{3h_1^2 h_2}{6} G^{(3)}_\varepsilon(x - h_0) + \frac{h_1^4}{24} G^{(4)}_\varepsilon(x - h_0).$$

Considering the expansion of $\xi(r) = \sum_{i\geq 0} c^i \xi_i(x)$, $\psi = \sum_{i\geq 0} c^i \psi_i$ and then comparing the SCF equations (10)–(13) at each order, we get the SCF equations at each order,

$$\omega_{Ai}(x) = \chi N \phi_{Bi}(x) - \xi_i(x) + \sum_{j=0}^{i} \psi_j G_{\varepsilon,i-j}(x - h_0), \tag{23}$$

$$\omega_{Bi}(x) = \chi N \phi_{Ai}(x) - \xi_i(x) - \sum_{j=0}^{i} \psi_j G_{\varepsilon,i-j}(x - h_0), \tag{24}$$

$$\phi_{Ai}(x) + \phi_{Bi}(x) = \delta_{0i}, \tag{25}$$

$$\int_{-\infty}^{\infty} \sum_{j=0}^{i} G_{\varepsilon,j}(x - h_0) \sum_{k=0}^{i-j} p_k(x)(\phi_{A,i-j-k}(x) - \phi_{B,i-j-k}(x))dx = 0. \tag{26}$$

Finally, the SCF equations are closed after we specify a criterion for the measurement of the bilayer curvature c. For a curved bilayer with a finite thickness, the definition of the interface position involves a certain degree of arbitrariness. In previous works,[17–19] the bilayer interface, r, is defined to be the midpoint of the two positions where A- and B-segment concentrations are equal, i.e., $\phi_A = \phi_B$. In this paper, for mathematical simplicity, we define the curvature of cylindrical and spherical bilayers as c, which satisfies the following equation:

$$\int \left(|\mathbf{r}| - \frac{1}{c}\right)\rho(\mathbf{r})d\mathbf{r} = \int_0^\infty r^n \left(r - \frac{1}{c}\right)\rho(r)dr = 0, \tag{27}$$

where $\rho(\mathbf{r})$ is regarded as a probability density function whose expectation is $1/c$. The choice of $\rho(\mathbf{r})$ is not unique. In this paper, we chose $\rho(\mathbf{r}) \propto \phi_B(\mathbf{r}) - f_B \phi_{bulk}$. It is worth noting that the definition of the interface affects the energy curve $F^C(c)$ and $F^S(c)$. We will discuss this effect in Sec. V A. Expanding $\rho(\mathbf{r})$ as $\rho(\mathbf{r}) = \sum_{i\geq 0} c^i \rho_i(x)$, we have the following constraints:

$$I_{\psi,i} := \sum_{j=0}^{i} \int_{-\infty}^{\infty} x p_j(x) \rho_{i-j}(x) dx = 0, \quad i = 0,1,2,\ldots, \tag{28}$$

where $p_0(x) = 1, p_1(x) = nx, p_2(x) = \frac{n(n-1)}{2}x^2, p_{i>2}(x) = 0$.

In summary, the self-consistent field equations at ith order contains (23)–(26) and (28). It is worth noting that there is no need to apply a constraint to stabilize the planar bilayers; hence, we have $\psi_0 = 0$. Consequently, h_0 can be directly determined by Eq. (26), i.e., $\int_{-\infty}^{\infty} G_{\varepsilon,0}(x - h_0)(\phi_{A,0}(x) - \phi_{B,0}(x))dx = 0$. Furthermore, the value of h_i for $i \geq 1$ can be directly determined by (26) once the SCF equations at jth order, $j < i$, are solved. The numerical method to solve the SCF equations will be introduced in Sec. IV.

C. Asymptotic expansion of the free energy

Once we solved the SCF equations at each order, the free energy of a bilayer can be calculated directly. Denote the semi-local excess energy density by $f(r)$,

$$f(r) = f_{bilayer}(r) - f_{bulk} = \sum_{i\geq 0} c^i f_i(x),$$

where $f_i(x)$ can be expressed as

$$\begin{aligned} f_i(x) = \sum_{k=0}^{i} [&\chi N \phi_{A,k}(x)\phi_{A,i-k}(x) \\ &- \omega_{A,k}(x)\phi_{A,i-k}(x) - \omega_{B,k}(x)\phi_{B,i-k}(x) \\ &- \xi_k(x)(\phi_{A,i-k}(x) + \phi_{B,i-k}(x) - \delta_{0,i-k})] \\ &- z_c q^+_{A,i}(x, f_A) - q^h_{A,i}(x, f_h) - \delta_{0i} f_{bulk}, \end{aligned}$$

then the excess energy density F_{ex} becomes

$$\begin{aligned} F_{ex} = \frac{1}{A}\int_V f(\mathbf{r})d\mathbf{r} &= c^n \int_0^\infty r^n f(r)dr \\ &= \int_{-1/c}^{\infty} (1 + cx)^n (f_0(x) + cf_1(x) + c^2 f_2(x) + \cdots)dx \\ &= \sum_{i\geq 0} c^i \int_{-\infty}^{\infty} dx \sum_{j=0}^{i} p_j(x) f_{i-j}(x) =: \sum_{i\geq 0} c^i F_i. \end{aligned}$$

Here, the integration domain is changed from $(-1/c, \infty)$ to $(-\infty, \infty)$ since c is small, the energy density decays very fast, and this modification only introduces negligible errors. In particular, we have the first three terms from the free energy expansion,

$$F_0 = \int_{-\infty}^{\infty} f_0(x)dx,$$

$$F_1 = \int_{-\infty}^{\infty} (f_1(x) + nxf_0(x))dx,$$

$$F_2 = \int_{-\infty}^{\infty} \left(f_2(x) + nxf_1(x) + \frac{n(n-1)}{2}x^2 f_0(x)\right)dx.$$

Denote the free energies of cylindrical and spherical bilayers (corresponding to $n = 1$ and $n = 2$, respectively) at ith order as F_i^C and F_i^S, respectively, then the elastic moduli can be directly calculated,

$$\kappa_M = 2F_2^C, \quad \kappa_G = F_2^S - 4F_2^C, \quad B_C = F_4^C, \quad B_S = F_4^S, \tag{29}$$

$$c_0 = -F_1^C/(2\kappa_M) = -F_1^S/(4\kappa_M), \quad \gamma = F_0 - 2\kappa_M c_0^2. \tag{30}$$

It is worth noting that $F^0 = F_0^C = F_0^S$ since they all correspond to the same SCF system related to the planar bilayers and $2F_1^C = F_1^S$ since the corresponding SCF systems only have a difference on the value n. However, there are no simple relations between the free energies at higher-orders, F_i, $i \geq 2$, because of nonlinearity. In addition, since we are considering bilayers consisting of two identical leaflets, the odd-order free energies are expected to be zeros, implying the spontaneous curvature $c_0 = 0$, due to the symmetry of the bilayers. Although the introduced constraint term $G_\varepsilon(\mathbf{r} - \mathbf{r}_1)$ will break this symmetry, its influence is limited, i.e., the odd-order energies F_i are small and negligible (less than 10^{-5} for the numerical results in Sec. V).

IV. NUMERICAL METHOD

Schematics of the numerical procedure to solve the SCF equations are shown in Fig. 2. For a given set of control parameters, the SCF equations are solved sequentially to obtain the structure and free energy of the bilayers at each order. Numerically, the SCF equations can be solved by iteration (Sec. IV B) during which one must compute the propagators by solving the modified diffusion equations (Sec. IV A) and store those propagators for more higher-order calculations.

Specifically, the computation domain is one-dimensional and limited to $x \in [-L, L]$, where the size L is determined by ensuring that the concentration profiles at the boundaries approach to the values of the bulk phase. We determine the length L via the decay length of $\phi_A^c(x)$ as shown in Fig. 1, where L_0 denotes the growth length, L_1 is the half-value length, and L_2 is the decay length at which the profile approaches its bulk value. The computation box size is then $L = L_0 + L_2$, which is large enough such that $L_2 \geq \lambda L_1$, where $\lambda = 4.5$ is chosen for our numerical examples. Besides, the MDEs are supplemented with reflecting boundary conditions. The number of spatial grid points is changed over 500–1000, and the number of time grid points is changed over 800–2000 under different model parameters to make sure that the free energy is converged in the order of 10^{-6} and the fields are self-consistent with L^2-norm error [the L^2-norm of the difference between the left-hand and right-hand sides of Eqs. (23)–(28)] less than 10^{-8}. We noted that the calculated elastic moduli (up to four orders) are not sensitive to the specific choices of the constraint width ε. The variances are less than 10^{-4} for ε changing from 0 Ω to 0.5 Ω, where Ω is the thickness of the bilayers. Therefore, in most of the calculations, we fix $\varepsilon = 0.25$ Ω.

A. Solve the MDEs

The MDEs [Eq. (18)] to be solved for the asymptotic expansion method are in the following generic form:

$$\frac{\partial}{\partial s}q(x,s) = a^2 \frac{\partial^2}{\partial x^2}q(x,s) - \omega(x)q(x,s) + g(x,s), \tag{31}$$

$$q(x,0) = q^0(x), \quad \frac{\partial}{\partial x}q(\pm L, s) = 0, \tag{32}$$

where $g(x, s)$ is a given source term. Since the fields and order-parameters change quickly near the bilayer interface and slowly near

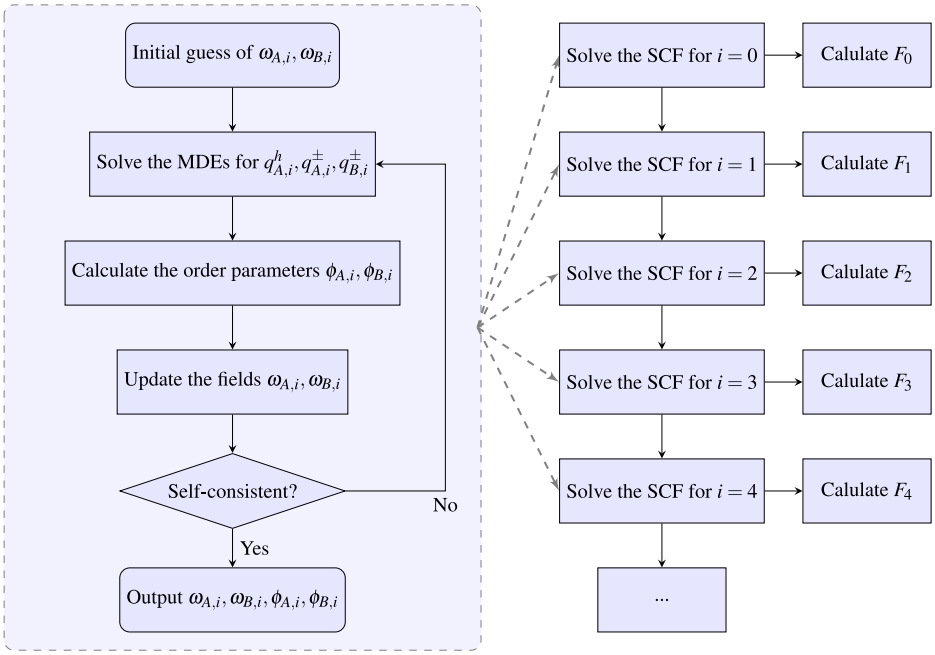

FIG. 2. Flowchart of the asymptotic expansion method.

the domain boundary, non-uniform grids for x are used to capture the details of the interfaces. The employed non-uniform grids correspond to a given transformation $x = t(\xi)$. With a proper change in variables, the MDE is changed but has the same form as Eq. (31), except with variable coefficients and the source term. In fact, let $t(\pm L) = \pm L$, $t''(\pm L) = 0$ and $q(x,s) = \sqrt{t'(\xi)}u(\xi,s)$, we have

$$\frac{\partial}{\partial s}u(\xi,s) = \tilde{a}^2(\xi)\frac{\partial^2}{\partial \xi^2}u(\xi,s) - \tilde{\omega}(\xi)u(\xi,s) + \tilde{g}(\xi,s), \tag{33}$$

$$u(\xi,0) = u^0(\xi), \quad \frac{\partial}{\partial \xi}u(\pm L,s) = 0, \tag{34}$$

where the new variables are

$$\tilde{a}^2(\xi) = \frac{a^2}{t'^2(\xi)},$$

$$\tilde{\omega}(\xi) = \omega(t(\xi)) - \frac{a^2}{2t'^4(\xi)}\left(t'(\xi)t'''(\xi) - \frac{3}{2}t''^2(\xi)\right),$$

$$\tilde{g}(\xi,s) = \sqrt{\frac{t(\xi)}{t'(\xi)}}g(t(\xi),s).$$

A valid transformation $t(\xi)$ is

$$t(\xi) = \xi + kL\left(\frac{1}{2\pi}\sin(2\pi\xi/L) - \frac{4}{\pi}\cos(\pi\xi_0/L)\sin(\pi\xi/L)\right),$$

where ξ_0 corresponds to the position of the bilayer interface, and k is a small positive number, such that $k \le 1/(2 + 4\cos^2(\pi\xi_0/L))$, which controls the non-uniform degree of the grid. A larger k results in a larger non-uniform degree, which means that more nodes are near the interface.

Using the Strang split method,[30] one can obtain the following two-order semi-discrete scheme for the differential equation (33):

$$u^{m+\frac{1}{2}}(\xi) = \exp(-\tilde{\omega}(\xi)\tfrac{\Delta s}{2})\left[u^m(\xi) + \tfrac{\Delta s}{8}(3\tilde{g}(\xi,s_m) + \tilde{g}(\xi,s_{m+1}))\right],$$

$$u^*(\xi) = \exp(-\tilde{a}^2(\xi)\Delta s\partial_\xi^2)u^{m+1/2}(\xi),$$

$$u^{m+1}(\xi) = \exp(-\tilde{\omega}(\xi)\tfrac{\Delta s}{2})u^*(\xi) + \tfrac{\Delta s}{8}(\tilde{g}(\xi,s_m) + 3\tilde{g}(\xi,s_{m+1})),$$

where $u^m(\xi)$ is the numerical approximation of $u(\xi, s_m)$, $s_m = m\Delta s$, and $u^*(\xi)$ can be solved by the well-known Crank–Nicolson scheme.[31]

It should be noted that the differential equations (31) and (33) could also be solved by using higher-order numerical schemes such as the compact finite-difference schemes.[32] In particular, if the partial derivative operators about x or ξ are treated by fourth-order compact finite-difference schemes, and the s dependence is dealt with by fourth-order Runge–Kutta methods,[33] then one could obtain fourth-order schemes finally.

B. Solve the SCF equations

Generally, the SCFT equations could be solved by using the Picard-type iteration,[20,34] where the fields, $\omega_{A,i}$ and $\omega_{B,i}$, are updated according to Eqs. (23) and (24), provided the Lagrange fields ξ_i and ψ_i are given. In detail, with old fields $\omega^{old}_{A,i}(x), \omega^{old}_{B,i}(x)$ [and its

corresponding concentrations $\phi_{A,i}^{old}(x), \phi_{B,i}^{old}(x)]$ in hand, one can update the fields by the iteration,

$$\omega_{A,i}^{new}(x) = (1-\alpha)\omega_{A,i}^{old}(x) + \alpha\left[\chi N\phi_{Bi}^{old}(x) - \xi_i^{old}(x) + \sum_{j=0}^{i}\psi_j^{old}G_{\varepsilon,i-j}(x-h_0)\right],$$

$$\omega_{B,i}^{new}(x) = (1-\alpha)\omega_{B,i}^{old}(x) + \alpha\left[\chi N\phi_{Ai}^{old}(x) - \xi_i^{old}(x) - \sum_{j=0}^{i}\psi_j^{old}G_{\varepsilon,i-j}(x-h_0)\right],$$

where α is an update ratio that was chosen as $\alpha = 0.01$ in our calculations. The Lagrange fields $\xi_i^{old}(x)$ and ψ_i^{old} are given by, omitted the superscript,

$$\xi_i(x) = \tfrac{1}{2}(\chi N(\phi_{Ai}(x)+\phi_{Bi}(x)) - (\omega_{Ai}(x)+\omega_{Bi}(x))) - \gamma\chi N(\phi_{Ai}(x)+\phi_{Bi}(x)-\delta_{0i}),$$

$$\psi_i = \frac{1}{2\int xG_\varepsilon(x-h_0)dx}\times\left[\int x(\omega_{Ai}(x)-\omega_{Bi}(x)-\chi N(\phi_{Bi}(x)-\phi_{Ai}(x)) - 2\sum_{j=0}^{i-1}\psi_j G_{\varepsilon,i-j}(x-h_0))dx - \beta\chi N I_{\psi,i}\right],$$

where γ, β are numerical parameters, which are chosen as $\gamma = 0.6$, $\beta = 0.4$. Note that the term $I_{\psi i}$ appeared in the iteration since the constraint (28) corresponds to the Lagrange multiplier ψ_i.

Although the Picard-type iteration is robust, it converges slowly. Accelerated methods such as the Anderson iteration[35] for the general fixed point problem could be used to solve the SCF equations,[36] resulting in the Anderson mixing technique. We start the Anderson iteration after the fields have been updated by Picard-type, with iterations reaching the point where the L^2-error of the SCF equations is less than 0.1.

V. RESULTS AND DISCUSSION

For simplicity, we focus on tensionless bilayer membranes where the activity or the chemical potential of the copolymers, z_c, is adjusted such that the excess free energy of a planar bilayer is zero, i.e., $F^0 = \gamma + 2\kappa_M c_0^2 = 0$, which is equivalent to $\gamma = 0$ since the spontaneous curvature c_0 is zero. Section V A presents numerical examples illustrating the two advantages of the asymptotic expansion method: (i) the consistency and efficiency compared to the polynomial fitting method and (ii) the analytic decompositions of the order-parameters. The analytic expressions of the asymptotic method permit us to access the elastic constants directly. Therefore, the proposed method provides an efficient method for the study of the dependence of the elastic properties on the molecular details, which is given in Sec. V B. Notably, in Sec. V C, we present a local approximation result for the Gaussian modulus κ_G.

A. The asymptotic expansion method

As the first step of our study, we compare the polynomial fitting method with the asymptotic expansion method proposed in this paper. Instead of directly comparing the elastic moduli, we compare the free energy curves of the cylindrical and spherical bilayers since the results of the polynomial fitting method will be affected by the maximal curvature used. Figure 3(a) shows an example of the free energy of the self-assembled tensionless cylindrical and spherical bilayers as functions of the curvature c. For the asymptotic expansion method, the second-order approximation F_2c^2 and the fourth-order approximation $F_2c^2 + F_4c^4$ of the free energies are given. The second-order approximation is not enough when c is large (such as $c = 0.25$), where the fourth-order approximation is more close to the free energy F_{ex}. It is worth noting that the fourth-order contribution to $F^S(c)$ is negative, while the overall contribution is small since there is an intrinsic limit due to the bilayer thickness on how high the curvature could be. In Fig. 3(b), we compare the fourth-order energy to the second-order energy for cylindrical and spherical bilayers with curvature $c = 0.15$. It indicates that for cylindrical bilayers with this mild curvature c, the fourth-order energy could be larger than 5% of the second-order energy, and this ratio is increasing with χN increasing or f_A decreasing. However, this ratio for spherical bilayers is relatively small. The consistency between the free energy F_{ex} and the approximations given by the asymptotic expansion method implies the efficiency of the asymptotic expansion method because one only needs to solve the SCF equations five times (three times memory) for the second-order free energies and additional four times (additional two times memory) for the fourth-order free energies.

Next, we illustrate another advantage of the asymptotic expansion method by decomposing the concentrations of cylindrical or spherical bilayers to each order. Figure 4 shows the profiles of the concentrations of a spherical bilayer with curvature $c \approx 1.4$ where the asymptotic expansion at each order is compared. Within the spherical bilayer, since the area of the inner interface is smaller than the outer one, the hydrophilic monomers (A-blocks) in the inner leaflet have to pack more closely and have a higher local concentration in comparison to the outer leaflet. This mechanism can be revealed by the trend of $\phi_{A,1}^c(x)$, which is almost an odd function and attains its maximum at the left part. Furthermore, the numerical results indicate that the odd-order terms are almost odd functions and the even-order terms are almost even functions. As a result, the odd-order energies such as F_1 and F_3 are close to zeros since terms in those integral are almost odd functions. For the example given in Fig. 4, both $|F_1|$ and $|F_3|$ are less than 10^{-6}.

It is worth noting that, in this paper, we adopt Eq. (27) to determine the bilayer interface, which is different from previous works.[17–19] Using the definition in Refs. 17–19, the curvature of cylindrical and spherical bilayers will have different values, denoted by $\tilde{c}$. Our numerical results indicate that the difference $\tilde{c} - c$ has order c^3 or $\tilde{c}^3$, i.e., $\tilde{c} - c \approx \sigma c^3 \approx \sigma\tilde{c}^3$, where α is a constant that can be estimated by remeasuring the interface. For example, for the spherical bilayers in Fig. 3, the estimated constant is $\sigma \approx 0.84$. In the asymptotic expansion method, remeasuring the interface can be done by restoring $\phi_A(r)$ and $\phi_B(r)$ from Eqs. (20)–(22). As a result, the second- and fourth-order energies of tensionless bilayers corresponding to $\tilde{c}$ are $\tilde{F}_2 = F_2, \tilde{F}_4 = F_4 - 2\sigma F_2$, which indicate that the second-order moduli

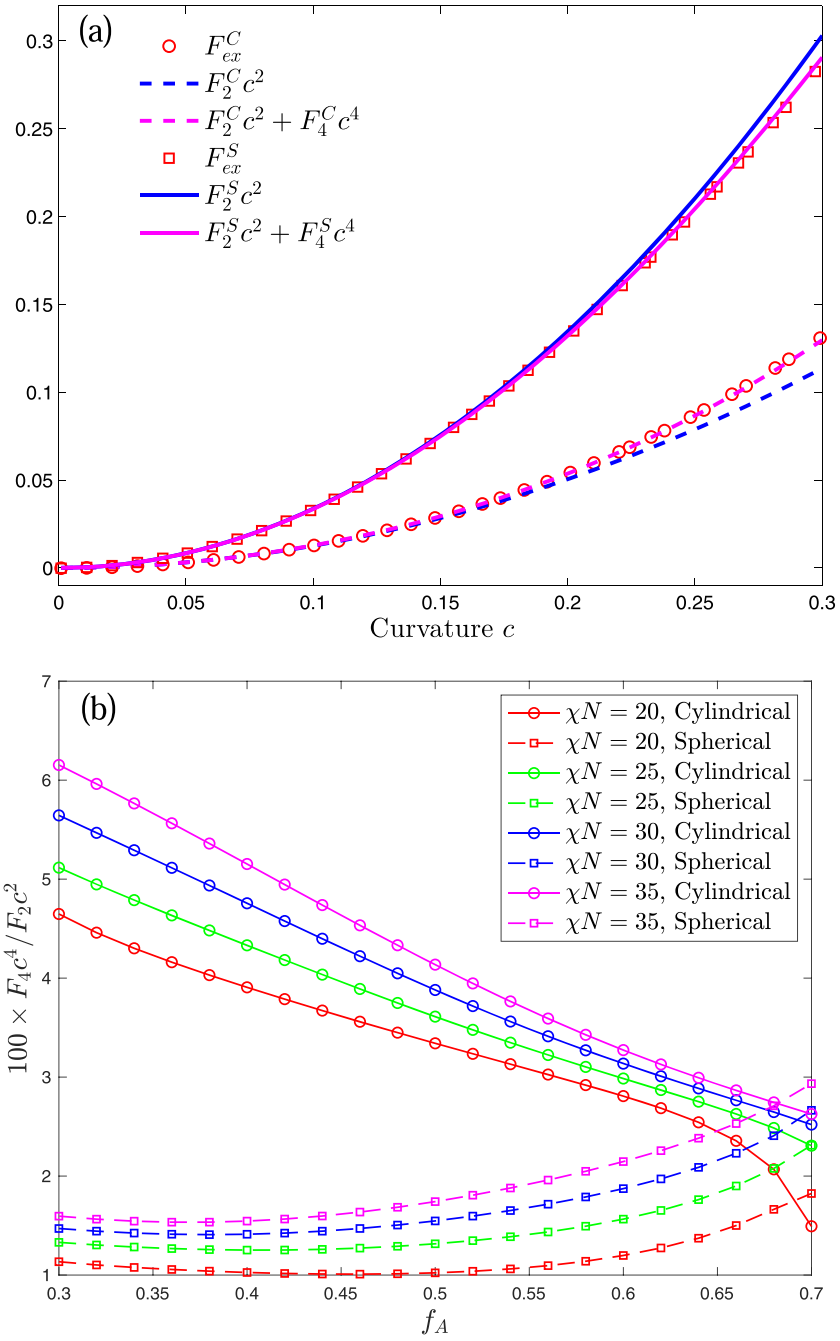

FIG. 3. [(a) and (b)] Comparison of the free energy of cylindrical and spherical bilayers. F_{ex} are calculated by the original constraint method, and F_2, F_4 are calculated by the method in this paper. *C* and *S* denote the cylindrical and spherical bilayers, respectively. The molecular parameters are $\chi N = 20$, $f_A = 0.5$, $f_h = 1$, and $b = 1$.

are independent of the definition of interface, but the fourth-order moduli are not.

B. Influence of interactions and amphiphilic architecture on the elastic moduli

Used the polynomial fitting method, previous studies[17] examined the effect of χN and f_A on the bending modulus κ_M and Gaussian modulus κ_G for the cases where both the copolymers and the homopolymers are assumed to have an equal chain length characterized by the same degree of polymerization, and both monomers (A and B) have the same statistical segment length, i.e., $f_h = 1$, $b = 1$. Those effects are reproduced in Fig. 5(a) where not only the second-order moduli (κ_M and κ_G) but also the fourth-order moduli (B_C and B_S) are given as functions of the hydrophilic fraction f_A. The main results are are as follows: (i) The bending modulus κ_M is

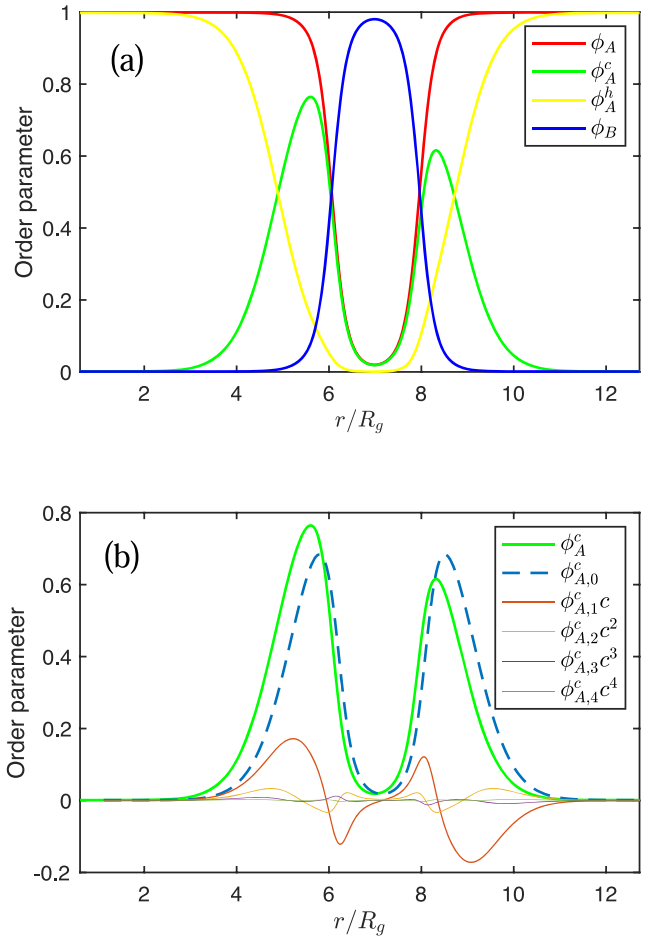

FIG. 4. (a) The order parameters of a spherical bilayer with curvature $c \approx 0.14$. (b) Decomposition of the order parameter ϕ_A. The molecular parameters are $\chi N = 20$, $f_A = 0.5$, $f_h = 1$, and $b = 1$.

not very sensitive to the amphiphilic architecture specified by f_A, and κ_M exhibits a weak symmetry to $f_A = 0.5$ (we will see later that this weak symmetry could be attributed to the assumption of equal statistical segment lengths of A and B). (ii) The Gaussian modulus κ_G is a monotonically decreasing function of f_A, and its value changes from positive to negative at around $f_A = 0.41$. (iii) The fourth-order modulus B_C is positive, but B_S is negative, and their magnitudes (or absolute value) are decreasing functions of f_A. (iv) The interaction χN mainly affects the magnitude of the moduli, where stronger interactions result in larger moduli, and this effect is almost linear to χN.

Figure 5(b) illustrates the influence of f_h on the elastic moduli as functions of f_A. The results are focused on four different values of $f_h \in \{0.6, 0.8, 1, 2\}$. It could be concluded that the moduli are less sensitive to the change in f_h. When f_h increases, the bending modulus slightly decreases and the Gaussian modulus increases. This weak influence of f_h is expected because the solubility of the amphiphilic molecules does not heavily depend on the length of the solvent homopolymers unless f_h is very small. In particular, shorter solvent homopolymers could help the amphiphilic molecules to be dissolved, resulting in a higher excess at the interface. The influence of increasing f_h on the fourth-order moduli is also small where the weak trend is that B_C decreases and B_S increases.

The effect of varying the geometrical asymmetry parameter b on the qualitative behavior of the elastic moduli is significant, as shown in Fig. 5(c) for different values of $b \in \{0.6, 0.8, 1, 1.2\}$. First of all, when b deviates from 1, the weak symmetry of κ_M to $f_A = 0.5$ is broken. When b increases, the magnitude of κ_M and κ_G increases and the f_A corresponding to the maximum of κ_M decreases. On the other hand, the increase in b will increase the magnitude of the fourth-order moduli and change the monotonicity of the fourth-order moduli with respect to f_A. For large b, both B_C and $|B_S|$ are monotonically decreasing with respect to f_A. However, when b is relatively small, the trend is similar to a unimodal function.

C. A local approximation for κ_G

An interesting observation is that the Gaussian modulus κ_G is zero at $f_A \approx 0.41$, independent of the value of χN, as illustrated in Fig. 5(a). We found that this phenomenon occurred in the cases of other parameters, as shown in Fig. 6. Specifically, the data shown in Fig. 6 by the gray thin curves revealed that, for a given set of parameters (f_h and b), the Gaussian modulus as a function of f_A crossed at a common point independent of the value of χN. Considering the Gaussian modulus κ_G as a function of f_A and χN, i.e., $\kappa_G(f_A, \chi N)$, and assuming that f_A is close to the crossover point f_A^*, one obtains the Taylor expansion with respect to f_A,

$$\kappa_G(f_A, \chi N) \approx \alpha(\chi N)(f_A - f_A^*) + \kappa_G(f_A^*, \chi N),$$

where $\alpha(\chi N)$ is the slope at the point that is a function of χN. The results shown in Fig. 6 suggest that at the cross point specified by f_A^*, the Gaussian modulus $\kappa_G(f_A^*, \chi N)$ is a constant κ_G^* that is independent of χN. Therefore, when f_A is close to f_A^*, one has the following approximation:

$$\kappa_G(f_A, \chi N) \approx \alpha(\chi N)(f_A - f_A^*) + \kappa_G^*. \tag{35}$$

We call (f_A^*, κ_G^*) *the cross point* and show the influence of f_h and b on (f_A^*, κ_G^*) in Fig. 6. The circles in Fig. 6 are the cross points corresponding to different parameters f_h and b and are joined to curves with the same $f_h = 1$ or $b = 1$. When f_h increases, both f_A^* and κ_G^* increase slightly. When b increases, f_A^* decreases but κ_G^* increases. The range of κ_G^* is large, which covers values from -1.1 to 6.2 in Fig. 6 where f_h changes from 0.3 to 5 and b changes from 0.3 to 1.8.

It is worth noting that f_A, f_h, and b are molecular parameters that do not depend on the temperature of the system, while the Flory–Huggins parameter χ does. Therefore, the approximation (35) suggests that we can control the molecular parameters to design a bilayer membrane whose Gaussian modulus is given and insensitive to the temperature. However, the planar bilayers are unstable if their Gaussian moduli are positive.[17] Therefore, Fig. 6 also indicates that large f_h and large b are harmful to this property because of their positive κ_G^*.

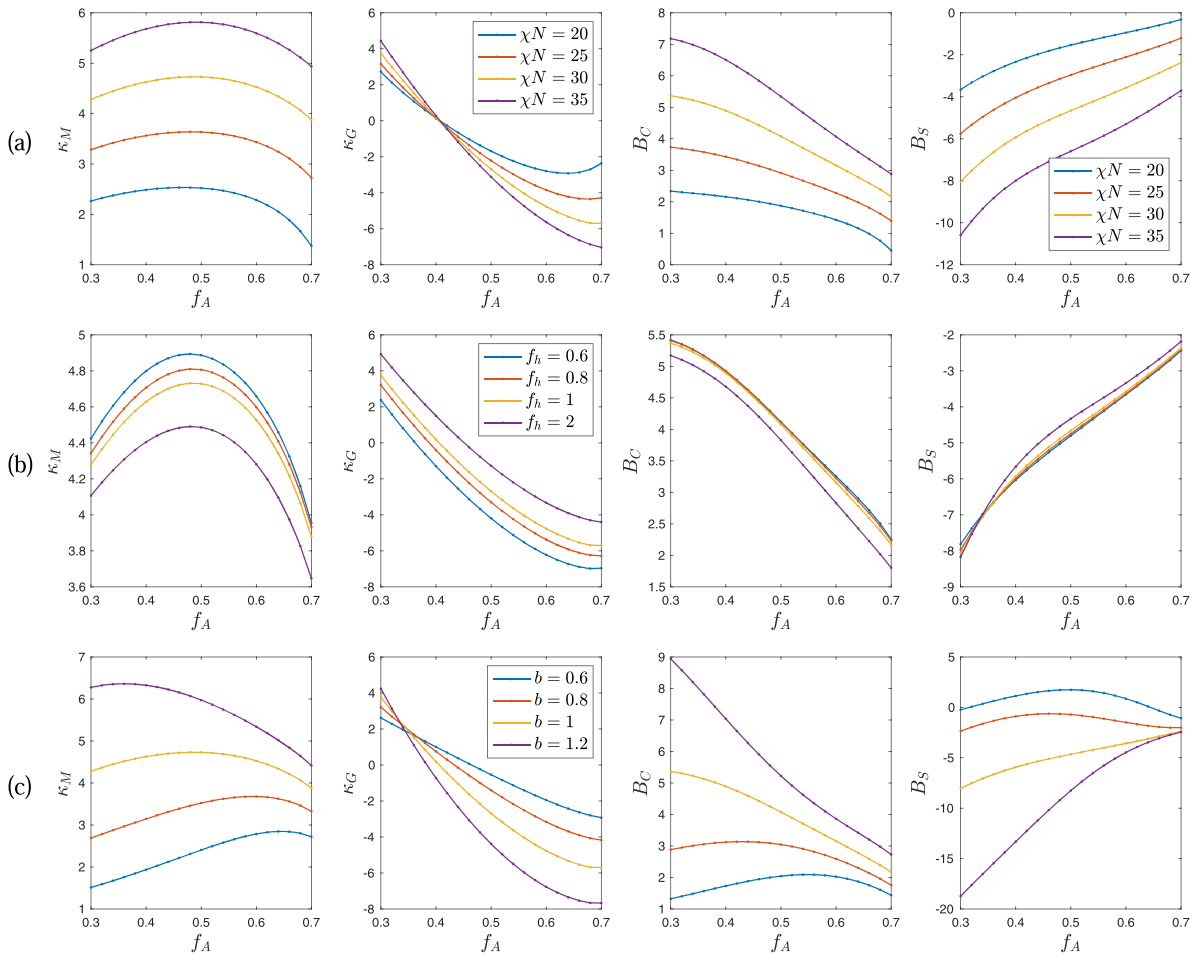

FIG. 5. The bending modulus κ_M, Gaussian modulus κ_G, and fourth-order moduli B_C and B_S of bilayer membranes as functions of the hydrophilic fraction f_A. The effect of (a) χN, (b) f_h, and (c) b on the moduli with a reference parameter $\chi N = 30$, $f_h = 1$, and $b = 1$.

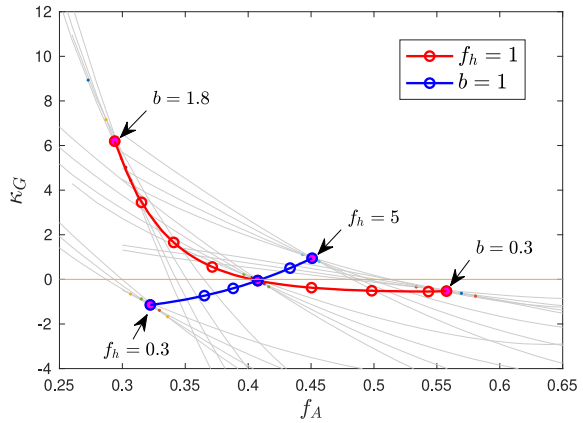

FIG. 6. Cross points of different parameters. The gray thin lines are the Gaussian modulus as functions of f_A for different $\chi N \in \{20, 25, 30, 35\}$. The circles are cross points corresponding to parameters $b \in \{0.3, 0.4, 0.6, 0.8, 1, 1.2, 1.4, 1.6, 1.8\}$ and $f_h \in \{0.3, 0.5, 0.7, 1, 2, 5\}$.

VI. CONCLUSION

In this paper, we proposed a novel method based on the asymptotic expansion theory using the curvature of the self-assembled bilayers as the expansion parameter, resulting in more accurate and efficient methods to calculate the elastic moduli of bilayer membranes. The method is presented within the framework of the self-consistent field theory, which is capable of accurately predicting the mechanical parameters of the self-assembled bilayer membranes. The curvature of the cylindrical and spherical bilayers is regarded as the small parameter in the asymptotic expansion methodology. The new method allows us to obtain analytic expressions of the elastic moduli of the self-assembled bilayer membranes. Compared with the existing polynomial fitting method, the asymptotic expansion method could be used to directly compute the elastic moduli by solving a series of self-consistent field equations. This allows us to design efficient numerical methods and pave the way to further understanding of the dependence of the elastic properties on the molecular architecture and microscopic parameters. Numerical examples verify the validity and efficiency of the proposed method.

Although the examined model is restricted to a coil–coil diblock system, it is straightforward to extend our method to other molecular architectures of flexible polymers characterized by the Gaussian-chain model, as well as non-polymeric systems. Future research will explore the extension to non-Gaussian models such as the wormlike-chain, which takes the orientational order into account.

ACKNOWLEDGMENTS

We thank Professor Pingwen Zhang for helpful discussions and anonymous reviewers for their valuable comments and useful suggestions. This research was supported by the NSF of China (Grant No. 11601099), the Science and Technology Foundation of Guizhou Province of China (Grant No. [2017]1032), and the Natural Science and Engineering Research Council (NSERC) of Canada.

DATA AVAILABILITY

The data that support the findings of this study are available from the corresponding author upon reasonable request.

REFERENCES

[1]B. M. Discher, Y. Y. Won, D. S. Ege, J. C. Lee, F. S. Bates, D. E. Discher, and D. A. Hammer, "Polymersomes: Tough vesicles made from diblock copolymers," Science **284**, 1143–1146 (1999).
[2]D. E. Discher and F. Ahmed, "Polymersomes," Annu. Rev. Biomed. Eng. **8**, 323–341 (2006).
[3]A. Taubert, A. Napoli, and W. Meier, "Self-assembly of reactive amphiphilic block copolymers as mimetics for biological membranes," Curr. Opin. Chem. Biol. **8**, 598–603 (2004).
[4]W. Helfrich *et al.*, "Elastic properties of lipid bilayers: Theory and possible experiments," Z. Naturforsch. C **28**, 693–703 (1973).
[5]Z. C. Tu and Z. C. Ou-Yang, "Recent theoretical advances in elasticity of membranes following Helfrich's spontaneous curvature model," Adv. Colloid Interface Sci. **208**, 66–75 (2014).
[6]J. F. Nagle, "Introductory lecture: Basic quantities in model biomembranes," Faraday Discuss. **161**, 11–29 (2013).
[7]R. Dimova, "Recent developments in the field of bending rigidity measurements on membranes," Adv. Colloid Interface Sci. **208**, 225–234 (2014).
[8]F. M. Thakkar, P. K. Maiti, V. Kumaran, and K. G. Ayappa, "Verifying scalings for bending rigidity of bilayer membranes using mesoscale models," Soft Matter **7**, 3963–3966 (2011).
[9]A. J. Sodt and R. W. Pastor, "Bending free energy from simulation: Correspondence of planar and inverse hexagonal lipid phases," Biophys. J. **104**, 2202–2211 (2013).
[10]M. Hu, J. J. Briguglio, and M. Deserno, "Determining the Gaussian curvature modulus of lipid membranes in simulations," Biophys. J. **102**, 1403–1410 (2012).
[11]A. Berthault, M. Werner, and V. A. Baulin, "Bridging molecular simulation models and elastic theories for amphiphilic membranes," J. Chem. Phys. **149**, 014902 (2018).
[12]D. Marsh, "Elastic curvature constants of lipid monolayers and bilayers," Chem. Phys. Lipids **144**, 146–159 (2006).
[13]P.-W. Zhang and A.-C. Shi, "Application of self-consistent field theory to self-assembled bilayer membranes," Chin. Phys. B **24**, 128707 (2015).
[14]B. Kheyfets, T. Galimzyanov, A. Drozdova, and S. Mukhin, "Analytical calculation of the lipid bilayer bending modulus," Phys. Rev. E **94**, 042415 (2016).
[15]M. Müller and G. Gompper, "Elastic properties of polymer interfaces: Aggregation of pure diblock, mixed diblock, and triblock copolymers," Phys. Rev. E **66**, 041805 (2002).
[16]K. Katsov, M. Müller, and M. Schick, "Field theoretic study of bilayer membrane fusion. I. Hemifusion mechanism," Biophys. J. **87**, 3277–3290 (2004).
[17]J. Li, K. Pastor, A.-C. Shi, F. Schmid, and J. Zhou, "Elastic properties and line tension of self-assembled bilayer membranes," Phys. Rev. E **88**, 012718 (2013).
[18]R. Xu, A. Dehghan, A.-C. Shi, and J. Zhou, "Elastic property of membranes self-assembled from diblock and triblock copolymers," Chem. Phys. Lipids **221**, 83–92 (2019).
[19]Y. Cai, P. Zhang, and A.-C. Shi, "Elastic properties of liquid-crystalline bilayers self-assembled from semiflexible–flexible diblock copolymers," Soft Matter **15**, 9215–9223 (2019).
[20]G. H. Fredrickson, *The Equilibrium Theory of Inhomogeneous Polymers* (Oxford University Press, Oxford, 2006).
[21]J. Zhou and A.-C. Shi, "Critical micelle concentration of micelles with different geometries in diblock copolymer/homopolymer blends," Macromol. Theory Simul. **20**, 690–699 (2011).
[22]I. Szleifer, D. Kramer, A. Ben-Shaul, W. M. Gelbart, and S. A. Safran, "Molecular theory of curvature elasticity in surfactant films," J. Chem. Phys. **92**, 6800–6817 (1990).
[23]G. Gompper and S. Zschocke, "Ginzburg-Landau theory of oil-water-surfactant mixtures," Phys. Rev. A **46**, 4836–4851 (1992).
[24]E. M. Blokhuis and D. Bedeaux, "Van der Waals theory of curved surfaces," Mol. Phys. **80**, 705–720 (1993).
[25]P. Flory, *Principles of Polymer Chemistry* (Cornell University Press, Ithaca, NY, 1953).
[26]M. Laradji and R. C. Desai, "Elastic properties of homopolymer-homopolymer interfaces containing diblock copolymers," J. Chem. Phys. **108**, 4662–4674 (1998).
[27]M. W. Matsen, "Elastic properties of a diblock copolymer monolayer and their relevance to bicontinuous microemulsion," J. Chem. Phys. **110**, 4658–4667 (1999).
[28]M. H. Holmes, *Introduction to Perturbation Methods* (Springer Science & Business Media, 2012), Vol. 20.
[29]J. C. Neu, *Singular Perturbation in the Physical Sciences* (American Mathematical Society, 2015), Vol. 167.
[30]G. Strang, "On the construction and comparison of difference schemes," SIAM J. Numer. Anal. **5**, 506–517 (1968).
[31]K. W. Morton and D. F. Mayers, *Numerical Solution of Partial Differential Equations: An Introduction*, 2nd ed. (Cambridge University Press, 2005).
[32]S. K. Lele, "Compact finite difference schemes with spectral-like resolution," J. Comput. Phys. **103**, 16–42 (1992).
[33]J. C. Butcher, *Numerical Methods for Ordinary Differential Equations*, 2nd ed. (Springer-Verlag, 2008).
[34]A.-C. Shi and J. Noolandi, "Effects of short diblocks at interfaces of strongly segregated long diblocks," Macromolecules **27**, 2936–2944 (1994).
[35]H. F. Walker and P. Ni, "Anderson acceleration for fixed-point iterations," SIAM J. Numer. Anal. **49**, 1715–1735 (2011).
[36]R. B. Thompson, K. O. Rasmussen, and T. Lookman, "Improved convergence in block copolymer self-consistent field theory by Anderson mixing," J. Chem. Phys. **120**, 31–34 (2004).